Journal of Neuropathology and Experimental Neurology
Issue: Volume 65(4), April 2006, pp 319-326

Publication Type: [Original Articles]
DOI: 10.1097/01.jnen.0000218442.07664.04
ISSN: 0022-3069
Accession: 00005072-200604000-00002
Keywords: Alzheimer disease, AMPA receptor, Atypical protein kinase C, Memory, Neurofibrillary tangle, Perisomatic granule, Synaptic plasticity

[Original Articles]

Atypical Protein Kinase C in Neurodegenerative Disease I: PKM[zeta] Aggregates With Limbic Neurofibrillary Tangles and AMPA Receptors in Alzheimer Disease

Crary, John F. PhD; Shao, Charles Y. MD, PhD; Mirra, Suzanne S. MD; Hernandez, A. Ivan PhD; Sacktor, Todd C. MD

Author Information

From the Graduate Program in Neural and Behavioral Science (JFC) and the Departments of Physiology and Pharmacology (JFC, AIH, TCS), Pathology (CYS, SSM), and Neurology (TCS), State University of New York Downstate Medical Center, Brooklyn, New York.

Send correspondence and reprint requests to: Suzanne S. Mirra, MD, Department of Pathology, Box 25, SUNY Downstate Medical Center, 450 Clarkson Avenue, Brooklyn, NY 11203; E-mail: suzanne.mirra@downstate.edu

Supported by NIH grants K07 AG 00959 (SSM), MH53576 (TCS) and MH57068 (TCS) with additional support from the Pine Family Foundation (JFC).

JFC and CYS contributed equally to this work.

Abstract

Protein kinase M[zeta] (PKM[zeta]), an atypical protein kinase C (PKC) isoform, plays a key role in the maintenance of long-term potentiation (LTP), a persistent enhancement of AMPA receptor-mediated synaptic transmission, as well as in the persistence of memory in *Drosophila*. Because memory impairment in Alzheimer disease (AD) has been attributed to disruption of synaptic plasticity, we investigated the expression and distribution of PKM[zeta] in this disorder. We found that PKM[zeta] accumulated in neurofibrillary tangles (NFTs), whereas conventional and novel PKC isoforms did not. Unlike tau, which is present in all NFTs regardless of location, PKM [zeta] was found in a subset of NFTs restricted to limbic or medial temporal lobe structures (i.e. hippocampal formation, entorhinal cortex, and amygdala), areas implicated in memory loss in AD. Interestingly, PKM[zeta] was not identified in any NFTs in control brains derived from 6 elderly individuals without known cognitive impairment. In medial temporal lobe structures in AD, PKM[zeta] also occurred within abnormal neurites expressing MAP2, GluR1 and GluR2 as well as in perisomatic granules expressing GluR1 and GluR2, suggesting that aggregation of PKM[zeta] disrupts glutamatergic

synaptic transmission. Together, these findings suggest a link between PKM[zeta]-mediated synaptic plasticity and memory impairment in AD.

INTRODUCTION

The limbic system, a group of associated structures involved in memory, is a site of early changes in Alzheimer disease (AD) (1-3). Although the mechanism underlying memory impairment in AD is not known, a failure of synaptic plasticity has been proposed (4). Specifically, long-term potentiation (LTP), a widely studied animal model of synaptic plasticity and memory, may be disrupted in AD. LTP can be mechanistically divided into 2 phases: a brief *induction* phase triggering synaptic enhancement, followed by a sustained *maintenance* phase, which may represent the physiological substrate of memory storage. Whereas many signaling events have been implicated in induction, including activation of postsynaptic NMDA receptors, increases in intracellular calcium, and stimulation of several protein kinases, the molecular mechanism of maintenance is not as well characterized (5). Recently, however, a specific protein kinase C (PKC) isoform, PKM[zeta], has been shown to be both necessary and sufficient for maintaining LTP (6).

Clarifying the role of PKC in memory function and dysfunction is complicated, in part, because the PKC family consists of 9 similar genes (7), each with distinct functions. The kinases encoded by these genes are classified by their cofactor activation profiles, which vary according to sequence differences in the kinase regulatory domains. Conventional PKC ([alpha], [beta], [gamma]) is activated by diacylglycerol (DAG) and calcium, novel PKC ([delta], [epsilon], [eta], [theta]) by DAG, and atypical PKC (aPKC; [zeta] and [iota]/[lambda]) is activated by other lipid second messengers and binding proteins, but not DAG and calcium (8). In general, cofactor binding to the autoinhibitory regulatory domain transiently activates PKC by inducing a conformational change in the enzyme, thus exposing the catalytic domain. In vitro, PKC also can be activated by proteolytic cleavage between the regulatory and catalytic domains, liberating an independent catalytic domain termed PKM. Free of regulatory domain inhibition, PKM phosphorylates substrates in the absence of cofactors. PKM[zeta], the only stable PKM form in the brain, is not, generated by partial proteolysis, but from a brain-specific PKM [zeta] mRNA transcribed from an internal promoter within the PKC[zeta] gene (9, 10). The PKM[zeta] mRNA is actively transported to dendrites (11) and translated during LTP maintenance (10). Because the PKM[zeta] message does not translate the autoinhibitory regulatory domain of PKC[zeta], PKM[zeta] is autonomously active, persistently phosphorylating substrates even in the absence of second messengers.

This persistent increase in PKM[zeta] is a critical core molecular mechanism for maintaining LTP in rodents. The increase in PKM[zeta] results in increased

phosphotransferase activity that causes and sustains an enhancement of alpha-amino-3-hydroxy-5-methyl-4-isoxazolepropionic acid (AMPA) receptor responses for hours (12). Recent work indicates that PKM[zeta] enhances AMPA receptor responses exclusively through regulation of receptor trafficking into the synapse (13). The role of PKM[zeta] in maintaining LTP appears specific because the activity of conventional PKC and novel PKC, or other kinases implicated in LTP induction, such as Ca^{2+}/calmodulin-dependent protein kinase II (CaMKII) and cAMP-dependent protein kinase, is not required during maintenance (6). Furthermore, experiments in *Drosophila melanogaster* show that overexpression of atypical PKM prolongs a simple form of classic conditioning, suggesting evolutionary conservation in memory storage (14).

The critical role of PKM[zeta] in synaptic plasticity prompted our study of the atypical PKC isoforms in AD brain. Although previous reports have documented the distribution of conventional PKC in AD (15, 16), the relationship of atypical PKC to AD neuropathology has not, to our knowledge, been studied. This article focuses on the expression and distribution of PKM[zeta] in AD, whereas an accompanying report highlights a second atypical PKC isoform, PKC[iota]/[lambda], and its expression in a spectrum of neurodegenerative disorders (17).

MATERIALS AND METHODS

Antibodies

Antibodies used in this study are listed in Table 1. The polyclonal antibodies against PKC isoforms ([alpha], [beta]II, [gamma], PKC[zeta] catalytic and aPKC C-terminal) were generated as previously reported (10, 18, 19). Briefly, peptides corresponding to the C-terminal regions of the PKC isoforms were synthesized (Quality Control Biochemicals, Hopkinton, MA). Additionally, a peptide within the catalytic domain of PKC[zeta], without homology to PKC[iota]/[lambda], was generated (10). The peptides were coupled to bovine serum albumin and injected intramuscularly into female New Zealand rabbits. After 1 to 3 boosts at 4-week intervals, rabbit antisera were affinity-purified on peptide-conjugated Sulpholink gel columns (Pierce, Rockford, IL). The mouse anti-PKC [iota] (human) and mouse anti-PKC[lambda] (rodent) both recognize human PKC[iota]/[lambda] protein and showed identical results in this study (Transduction Laboratories, Lexington, KY). Thus, these antisera are referred to collectively as "anti-PKC[iota]/[lambda]" in this article.

Antigen	Dilution	Type	Source
Atypical PKC antibodies (immunohistochemistry and Western blot)			
PKCζ-catalytic	1:250	Polyclonal	Sacktor Laboratory (10, 18, 19)
PKCι/λ-catalytic	1:250	Monoclonal	Transduction Laboratory, Lexington, KY
aPKC C-terminal	1:250	Polyclonal	Sacktor Laboratory (10, 18, 19)
Conventional and novel PKC antibodies (immunohistochemistry)			
PKCα	1:500	Polyclonal	Sacktor Laboratory (10, 18, 19)
PKCβI (clone E3)	1:100	Monoclonal	Santa Cruz Biotech., Santa Cruz, CA
PKCβII	1:200	Polyclonal	Sacktor Laboratory (10, 18, 19)
PKCγ	1:500	Polyclonal	Sacktor Laboratory (10, 18, 19)
PKCδ (clone G9)	1:25	Monoclonal	Santa Cruz Biotechnology
PKCε (clone E-5)	1:100	Monoclonal	Santa Cruz Biotechnology
PKCη	1:10	Polyclonal	Santa Cruz Biotechnology
PKCΘ (clone E7)	1:10	Monoclonal	Santa Cruz Biotechnology
Other antibodies (immunohistochemistry)			
PHF1	1:100	Monoclonal	Provided by Dr. Peter Davies (28)
MAP2	1:100	Monoclonal	Chemicon International, Temecula, CA
GluR1	1:100	Monoclonal	Santa Cruz Biotechnology
GluR2	1:100	Monoclonal	Chemicon International

TABLE 1. Antibodies

Case Material

Autopsy brain tissue was derived from 8 patients with neuropathologically confirmed AD (20, 21) and 6 individuals (controls) with no known history of dementia (Table 2). The mean age of death of the AD group was 78.4 years (range, 60-91 years) and that of the controls was 75.7 years (range, 60-98 years). As expected in an elderly cohort, neurofibrillary changes were observed in a restricted distribution in the 6 control cases; none of the controls, however, met neuropathologic criteria for the diagnosis of AD (20, 21). Paraffin sections (8 μm) of hippocampus, amygdala, frontal cortex, temporal cortex, parietal cortex, occipital cortex, nucleus basalis, midbrain including dorsal raphe, and pons including locus ceruleus were used for immunohistochemistry. The postmortem intervals (PMI) on 7 AD and 4 control cases ranged from 1.5 to 14 hours (the PMI was not available on one AD and 2 control cases).

Case No.	Age	Sex	Braak Stage (1)	Diagnosis	Postmortem Interval (hr)
1	60	F	VI	AD	NA
2	72	F	VI	AD	4.0
3	82	M	V	AD	2.5
4	70	F	V	AD	1.5
5	86	F	V	AD	6.5
6	91	F	IV/V	AD	3.0
7	83	F	IV	AD	3.5
8	83	F	IV	AD	14.0
9	65	M	III–IV	Control	12.0
10	96	F	III–IV	Control	NA
11	66	F	II	Control	NA
12	69	M	II	Control	6.0
13	98	M	II	Control	NA
14	60	F	I	Control	8.0

NA, not available; AD, cases meeting neuropathologic criteria for Alzheimer disease (20, 21); Control, no known history of dementia without neuropathologic criteria for Alzheimer disease.

TABLE 2. Autopsy Case Material

For Western blot, fresh-frozen autopsy brain tissue was derived from 4 individuals with a mean age of 83 years (range, 72-88 years) without neurologic disease or neuropathology (provided by the Rush Alzheimer's Disease Center, Chicago, IL). The PMI of these 4 cases ranged from 3 to 7 hours.

Immunoblotting

Brain tissue from hippocampus, caudate nucleus, and gray and white matter from superior temporal cortex and cerebellum were homogenized in buffer (50 mM 4-[2-hydroxyethyl]-1-piperazineethanesulfonic acid [HEPES] [pH 7.5], 5 mM ethylene diamine tetra-acetic acid [EDTA], 5 mM ethylenebis[oxyethylenenitrilo]tetraacetic acid [EGTA], 5 mM 2-mercaptoethanol) containing protease inhibitors (0.1 mM phenylmethylsulfonyl fluoride, 17 kallikrein U/mL aprotinin, 5 mM benzamidine, 0.1 mM leupeptin) and phosphatase inhibitors (50 mM sodium fluoride, 40 mM [beta]-glycerol phosphate, 10 mM

pyrophosphate). Protein concentration was measured by bicinchoninic acid assay (Pierce). Fifteen micrograms of total protein was subjected to SDS-polyacrylamide gel electrophoresis (SDS-PAGE), transferred to nitrocellulose, probed with isoform-specific antisera for 1 hour, and developed with BCIP/NBT as described previously (18).

To assess the postmortem stability of PKM[zeta], levels within hippocampus were measured in 1-month-old Sprague-Dawley rats (n = 16) using quantitative immunoblots at PMIs ranging from 1 to 24 hours. The brains were kept at 4°C. Two additional rat brains were examined at 48 hours after storage at room temperature. No diminution in the level of PKM[zeta] was observed over time (data not shown), indicating stability of the protein.

Immunohistochemistry and Confocal Laser Microscopy

Paraffin-embedded sections (8 μm) were submerged in 10 mM citrate buffer (pH 6.0) and microwaved for 5 minutes. Slides were rinsed in phosphate-buffered saline (PBS) for 5 minutes, treated with 99% formic acid for 2 minutes, and rinsed in PBS. Sections were treated with 3% hydrogen peroxide for 10 minutes, rinsed in PBS for 5 minutes, blocked in 4% normal horse serum for 20 minutes, and incubated in primary antibody in a humidity chamber overnight. Sections then were rinsed in 2 changes of PBS for 10 minutes each and developed using the ABC system (Vector Laboratories, Burlingame, CA), which yields a dark brown reaction product, as described previously (19). Sections were rinsed in water, counterstained with Gill's hematoxylin for 5 minutes, rinsed twice, dipped in bluing solution 10 times, rinsed again, dehydrated, and coverslipped. For controls, sections were treated as previously mentioned with omission of primary antisera or with antisera preincubated for 1 hour with the immunizing peptide at a concentration of 10 μg/mL. As an additional control, sections were incubated in serum (1:200) from the rabbit from which the antisera was derived before immunization.

For quantification of the proportion of aPKC-positive NFTs, some sections were incubated with PHF1 after labeling with specific aPKC antisera, rinsed, incubated in biotinylated secondary (1:200), rinsed, incubated in ABC reagent, and developed with the VECTOR VIP substrate kit (Vector Laboratories), which yields a purple reaction product. The proportion of aPKC-positive NFTs was determined by dividing the number of aPKC-positive NFTs (dark brown reaction product) by the total number of NFTs as determined by PHF1-positivity in 3 20× fields of maximum tangle density in CA1-subiculum, entorhinal cortex, amygdala, midfrontal gyrus, and superior temporal gyrus.

For confocal microscopy, sections were incubated in fluorescein isothiocyanate (FITC)-conjugated donkey antirabbit (1:200) and tetramethyl rhodamine isothiocyanate (TRITC)-conjugated donkey antimouse (1:500; Jackson ImmunoResearch Laboratories, West Grove, PA) for 1 hour after incubation in primary antisera. To minimize nonspecific

label, these secondary antibodies had been solid phase-adsorbed by the vendor against a panel of nontarget antibodies derived from other species. To reduce background immunofluorescence, sections were then treated with Sudan black as described (22). Sections were then imaged using a MRC 1024 ES confocal microscope with a krypton /argon laser and analyzed using LaserSharp 2000 (Bio-Rad Laboratories, Hercules, CA). To confirm fluorescent channel specificity, parallel sections treated under identical conditions, except for omission of each primary antibody, were evaluated.

RESULTS

Immunoblot Findings

We first confirmed that normal human brain derived from elderly individuals without neurologic disease expresses PKM[zeta]. Western blots with [zeta]-specific catalytic domain antisera showed a prominent band at 55 kD corresponding to PKM[zeta] in the hippocampus, caudate nucleus, superior temporal cortex, and cerebellum (Fig. 1A). The cerebellum displayed an additional species at 72 kD corresponding to full-length PKC[zeta]. This predominance of PKM[zeta] in forebrain of adult humans is identical to its distribution in rat brain (10). A third minor band was inconsistently observed at 63 kD. The other closely related aPKC, PKC[iota]/[lambda] (the amino acid sequences of the human PKC[iota]/[lambda] catalytic domain and human PKM[zeta] are 83.8% identical), was also expressed in all brain regions tested (Fig. 1B). Consistent with work in rats (10), no truncated PKM form of this isozyme was observed. An antiserum targeting the C-terminus of PKM[zeta] that also recognizes PKC[iota]/[lambda] confirmed the presence of these isoforms in human brain (Fig. 1C). Hence, the distribution of the atypical PKC isoforms in human brain parallels that seen in rodents with PKM[zeta] being the predominant product of the [zeta] gene in forebrain (10).

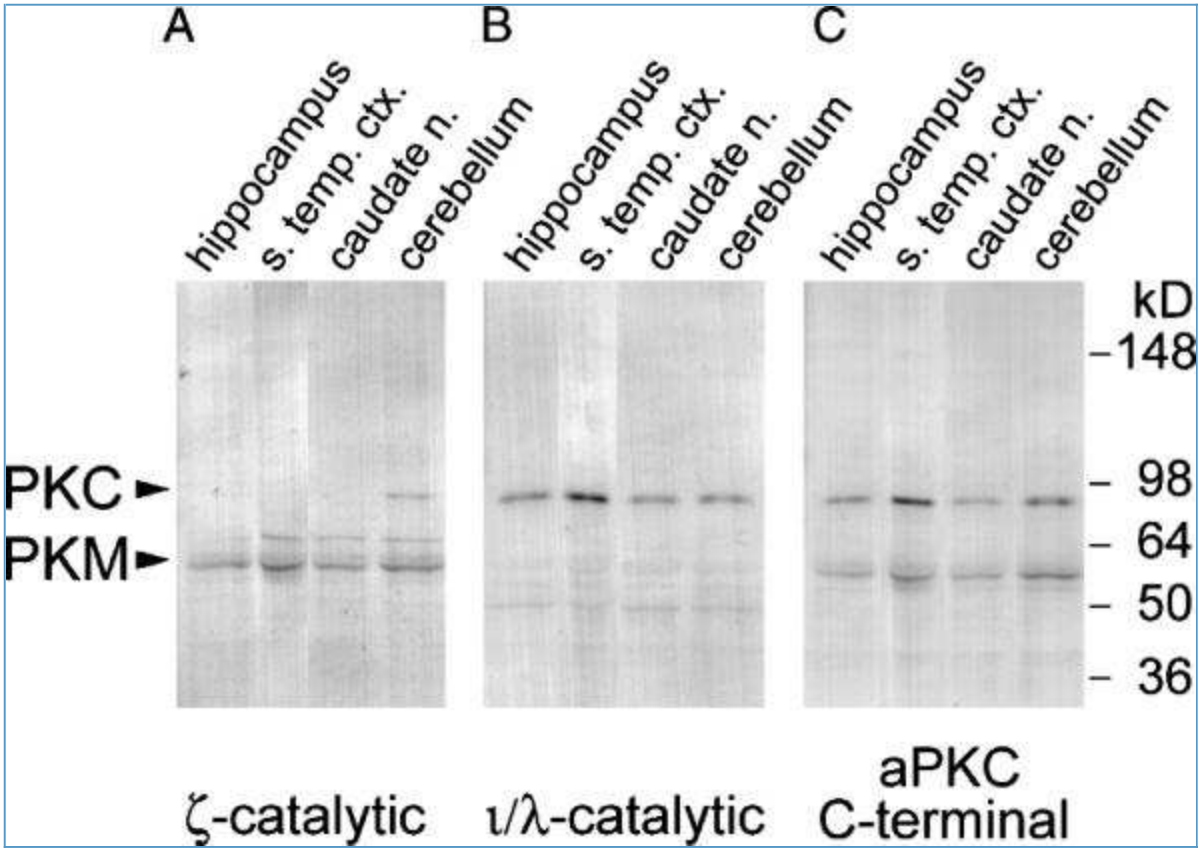

FIGURE 1. Expression of aPKC in human brain. A representative immunoblot of hippocampus, superior temporal cortex, caudate nucleus, and cerebellum derived from patients without known neurologic disease is shown. **(A)** Antibody to the [zeta]-catalytic domain detects a major band at 55 kD, corresponding to PKM[zeta], in all 4 regions. In contrast, full-length PKC[zeta] (72 kD) is present only in the cerebellum. **(B)** Antibody to the catalytic domain of PKC[iota]/[lambda] (72 kD) demonstrates expression of this aPKC isoform in all regions tested. **(C)** Antibody to the aPKC C-terminus, recognizing both PKC[iota]/[lambda] and PKM[zeta], confirms expression of these gene products in all regions tested.

Immunohistochemical Findings

PKM[zeta] immunopositivity was found in a subset of NFTs within medial temporal lobe structures (Fig. 2A, B; Table 3), i.e. hippocampus, entorhinal cortex, subiculum, and amygdala. These NFTs were recognized based on their typical fibrillary nature and flame-shaped appearance. Moreover, the PKM[zeta]-immunopositive structures were present in cells exhibiting NFTs on adjacent sections of the same blocks. Interestingly, no PKM[zeta]-containing NFTs were observed in tangle-containing regions outside the limbic system, i.e. frontal, parietal, and occipital neocortex, striatum, nucleus basalis, dorsal raphe nucleus, and locus ceruleus. In contrast, PKC[iota]/[lambda] was found in NFTs in all these regions, whether limbic or extralimbic (Fig. 2C, D). Antibodies against both aPKC isoforms revealed modest, finely granular cytoplasmic immunopositivity within neurons throughout the brain in a manner similar to that described in rodents

(19). Senile plaques, on the other hand, failed to label with either antibody.

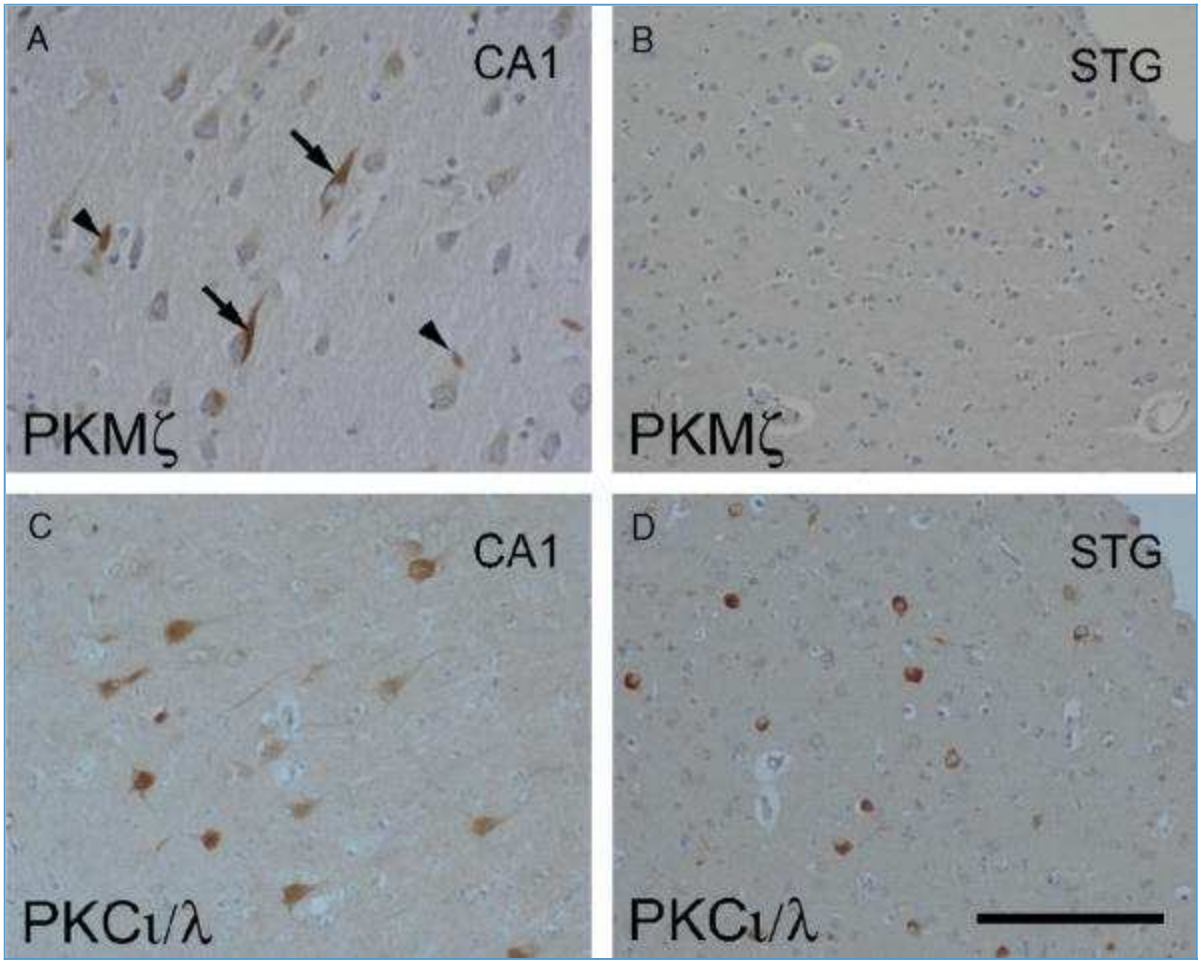

FIGURE 2. Two atypical PKC isoforms, PKM[zeta] and PKC[iota]/[lambda], are present within neurofibrillary tangles (NFTs) in Alzheimer disease. PKM[zeta] immunopositivity is restricted to NFTs within limbic regions; PKC[iota]/[lambda] antibody labeled NFTs throughout the brain. **(A)** Two NFTs in CA1 pyramidal cells of the hippocampus exhibit PKM[zeta] immunopositivity (arrows). Hirano bodies (arrowheads) are also PKM[zeta]-positive. Less intense granular cytoplasmic label is seen in neighboring unaffected neurons. **(B)** PKM[zeta] antibody fails to label NFTs outside of the limbic system. Superior temporal gyrus (STG). **(C)** Multiple PKC[iota]/[lambda]-immunoreactive NFTs are seen within the pyramidal cell layer of CA1. **(D)** In contrast to PKM[zeta], PKC[iota]/[lambda]-immunoreactive NFTs are common within extralimbic structures. Superior temporal gyrus (STG). **(A, C)** Scale bar = 90 μm; **(B, D)** scale bar = 180 μm.

	Case No.							
	1	2	3	4	5	6	7	8
Limbic system								
CA1	+	+	+	−	+	+	+	+
Subiculum	+	+	+	−	+	+	−	+
Entorhinal Cortex	+	+	−	−	−	+	−	+
Amygdala	+	+	+	+	−	+	NA	+
Projection nuclei								
Nucleus basalis	−	−	−	−	−	−	−	−
Dorsal raphe	−	−	NA	−	−	−	−	−
Locus ceruleus	−	−	−	−	−	−	−	−
Cerebral cortex								
Frontal	−	−	−	−	−	−	−	−
Temporal	−	−	−	−	−	−	−	−
Parietal	−	−	−	−	−	−	−	−
Occipital	−	−	−	−	−	−	−	−

NA, not available; (+/−) indicates the presence or absence of PKMζ-positive neurofibrillary tangles.

TABLE 3. Distribution of PKM[zeta]-Positive Neurofibrillary Tangles

Within limbic structures, PKM[zeta] immunolabeling identified a subset of tangle-bearing neurons (Table 4). Ghost or extracellular tangles were not immunoreactive for PKM[zeta] (data not shown). Double-labeling experiments with PHF1 confirmed the presence of PKM[zeta] in NFT-bearing neurons (Fig. 3A-C). The accumulation of PKC in tangles was specific to the aPKC subclass. NFTs failed to label with antibodies to isoforms of conventional PKC, confirming previous reports (15, 16). NFTs also were immunonegative using antibodies to novel PKC (data not shown).

	PKMζ	PKCι/λ
CA1/subiculum	12% ± 15	44% ± 24
Entorhinal cortex	24% ± 30	72% ± 14
Amygdala	25% ± 36	50% ± 24
Middle frontal cortex	Rare	81% ± 13
Superior temporal cortex	Rare	78% ± 18

*, Mean percentage ± standard error of the mean.

TABLE 4. Proportion of aPKC-Positive Neurofibrillary Tangles in Different Brain Regions in Alzheimer Disease*

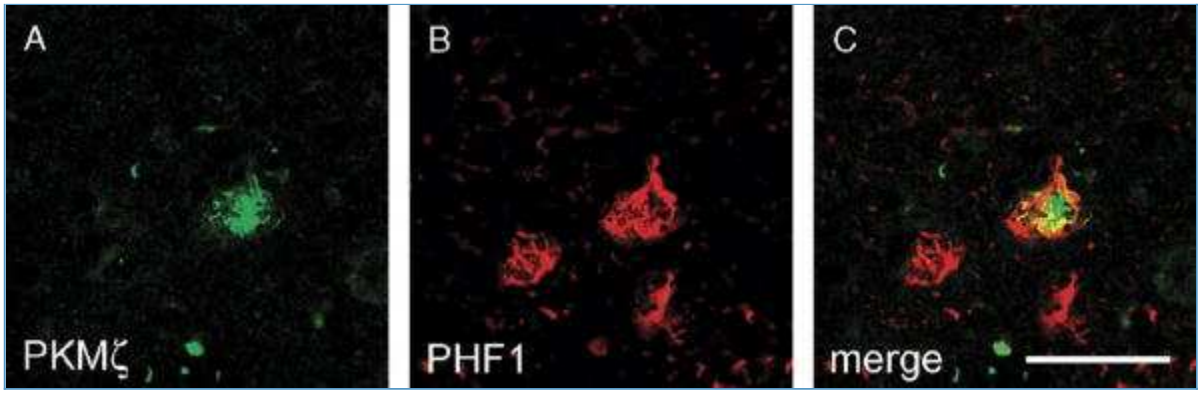

FIGURE 3. Confocal microscopy demonstrates that PKM[zeta] colocalizes with PHF1 in a subset of neurofibrillary tangles within limbic regions in Alzheimer disease. **(A-C)** PKM [zeta] immunofluorescence (green) is demonstrated in one of 3 PHF1-positive tangles (**B**, red) in the subiculum, as seen in the merged image **(C)**. PKM[zeta] label exhibits partial overlap (yellow) with PHF1. Single confocal z-plane, scale bar = 40 μm.

Prominent PKM[zeta] label of nonplaque-associated distended neurites was variably observed in the limbic regions containing PKM[zeta]-positive tangles (Fig. 4); many of these neurites were negative for PHF1 (Fig. 5A-C). PKM[zeta] also colocalized with the dendritic marker MAP2 (Fig. 5D-F), supporting the dendritic nature of these neurites.

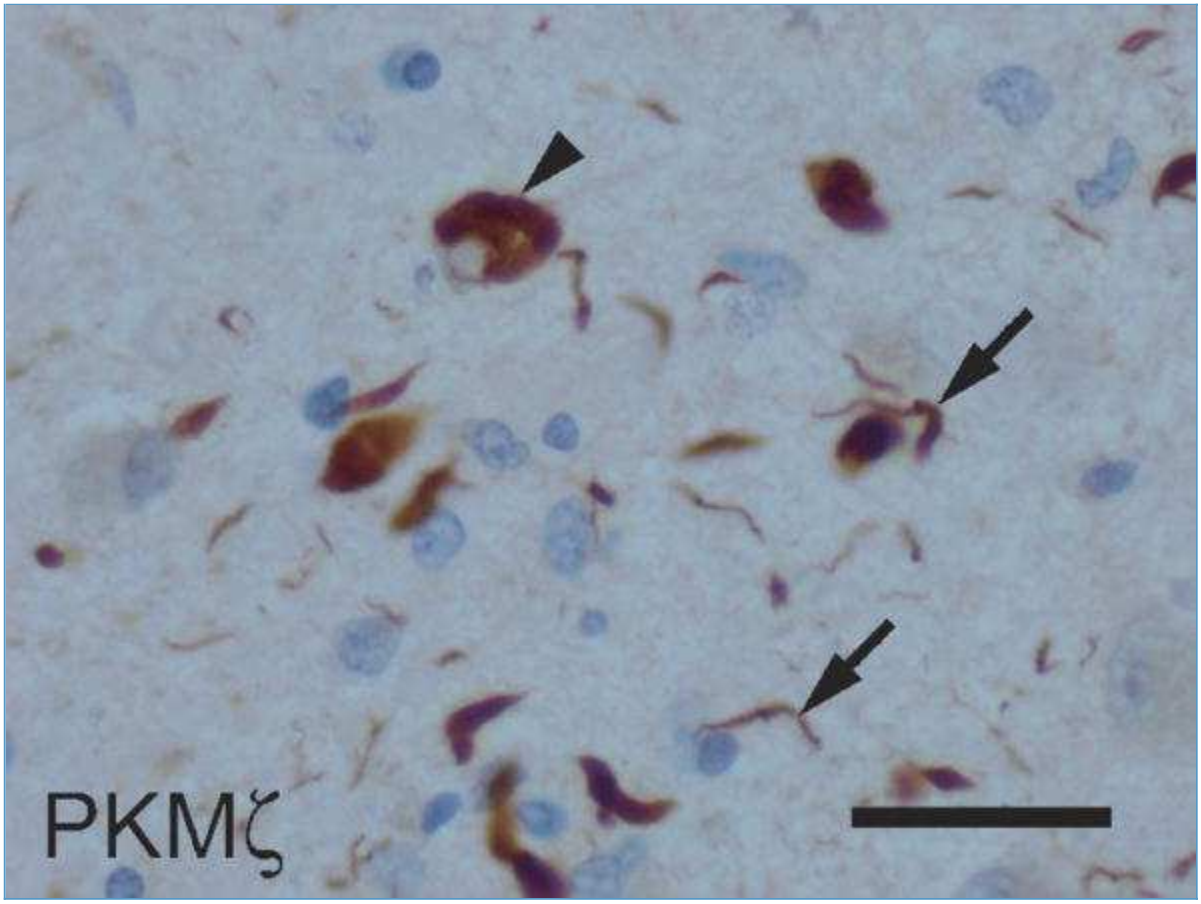

FIGURE 4. PKM[zeta] antibody labels neurites (arrows) as well as neurofibrillary tangles (arrowhead) within limbic structures. Amygdala. Scale bar = 40 µm.

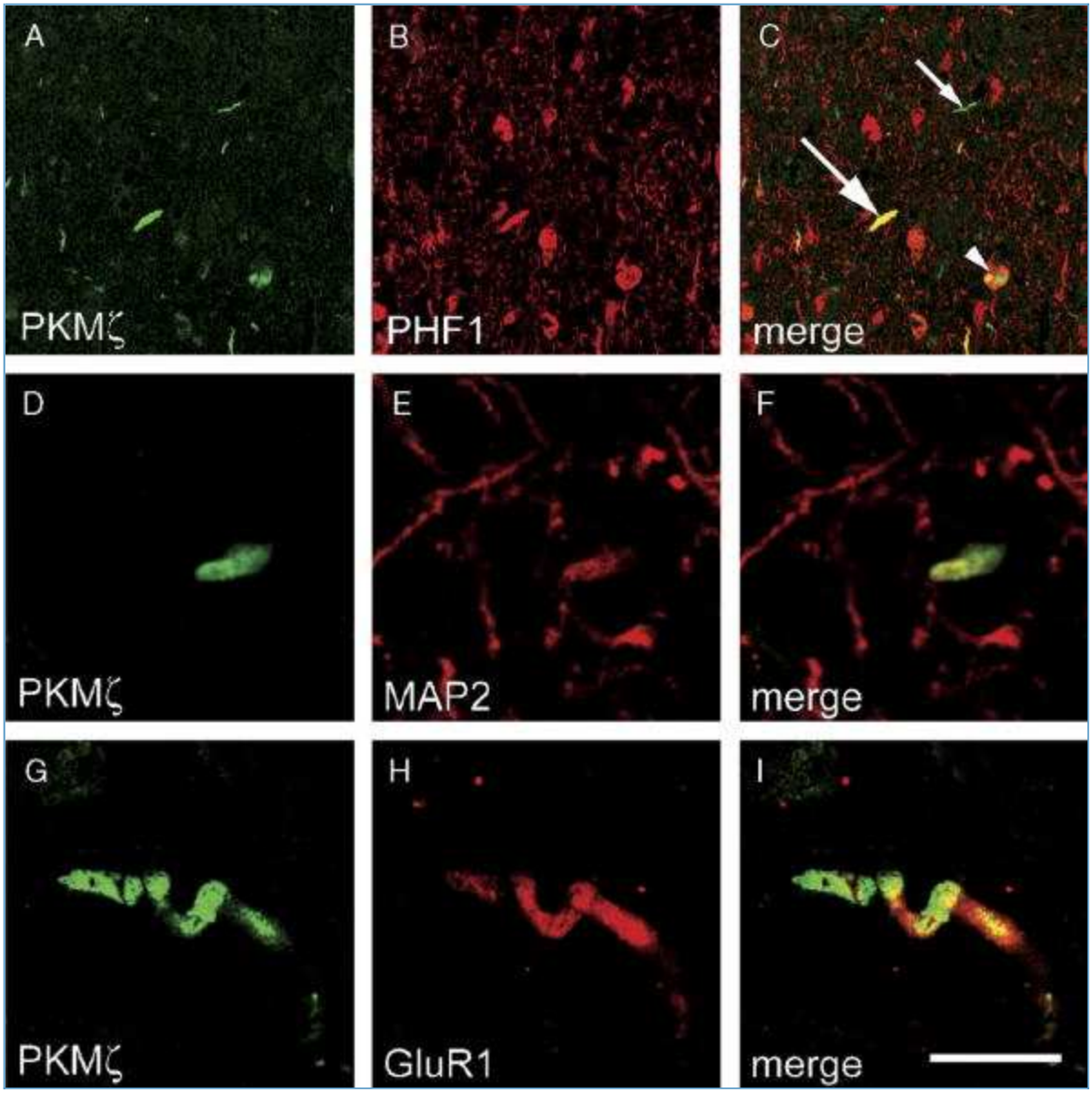

FIGURE 5. Confocal microscopy of PKM[zeta]-immunoreactive neurites in Alzheimer disease showing colocalization with PHF1, the dendritic marker, MAP2, and GluR1. **(A-C)** PKM[zeta] (**A**, green) and PHF1 (**B**, red) colocalize (yellow) in neurites as seen in merged image (**C**, large arrow). Some PKM[zeta]-positive neurites, however, are PHF1-negative (small arrow). A single PKM[zeta]-positive neurofibrillary tangle (arrowhead) is observed. Subiculum. **(D-F)** Colocalization of PKM[zeta] and MAP2 is seen in a thickened dendrite. Subiculum. **(G-I)** A neurite with a corkscrew configuration in the subiculum demonstrates colocalization of PKM[zeta] and GluR1. Amygdala. Images represent a single confocal z-plane. **(A-C)** Scale bar = 100 µm; **(D-F)** scale bar = 30 µM; **(G-I)** scale bar = 12.5 µM.

Given PKM[zeta]'s role in modulating AMPA receptors at synapses during maintenance of LTP, we examined the relationship of PKM[zeta] to the AMPA receptor

subunits GluR1 and GluR2 in AD. These antisera labeled some of the PKM[zeta]-positive dendrites (Fig. 5G-I) and perisomatic granules around CA1 neurons in the hippocampus (Fig. 6A), consistent with previous reports (25, 26). Interestingly, PKM [zeta] also labeled some of these granules; Hirano bodies also were immunoreactive (Fig. 6B-E).

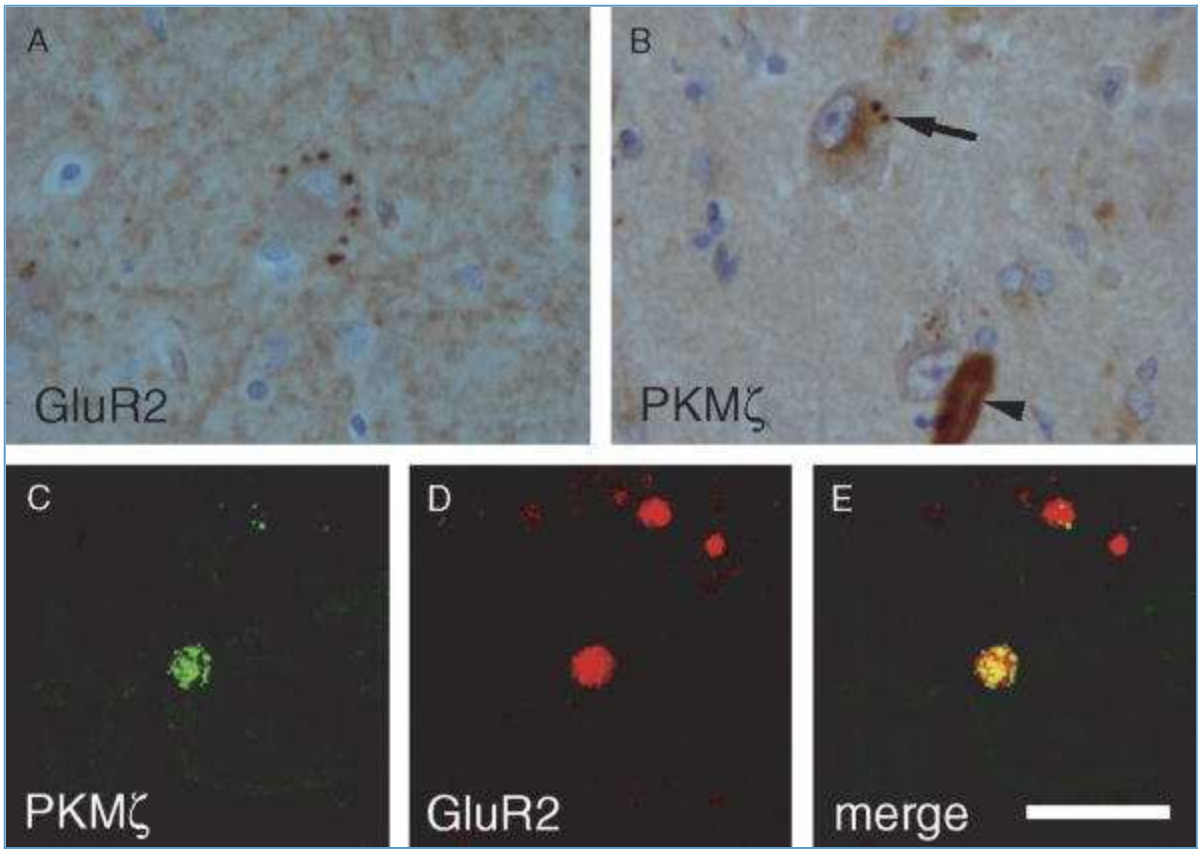

FIGURE 6. Perisomatic granules in CA1 pyramidal cells contain PKM[zeta] and GluR2. **(A)** GluR2 antibody labels perisomatic granules. Immunoperoxidase. **(B)** Perisomatic granules are also PKM[zeta]-immunoreactive as is a Hirano body (arrowhead). **(C-E)** Confocal microscopy demonstrates PKM[zeta] (green) and GluR2 (red) immunofluorescence with colocalization (yellow) in one granule. **(A, B)** Scale bar = 100 μM; **(C-E)** scale bar = 20 μm; images represent a single confocal z-plane.

We then examined autopsy brains derived from elderly individuals with no known history of dementia (n = 5; case no. 13 was excluded because of limited tissue availability). Although these cases failed to meet the neuropathologic diagnosis of AD, they all exhibited sparse to moderate numbers of NFTs in the entorhinal cortex, with 4 of the 5 cases also exhibiting sparse to moderate NFTs in the hippocampus, as is commonly encountered in normal elderly subjects without dementia (2). In contrast to the AD cases in which some NFTs exhibited PKM[zeta] immunoreactivity, no PKM[zeta] aggregation was observed within the NFTs in the normal elderly subjects without dementia, i.e. control cases (Fig. 7A). PKC[iota]/[lambda] immunolabeling, however, was observed in entorhinal tangles in 3 of the 5 control brains (Fig. 7B).

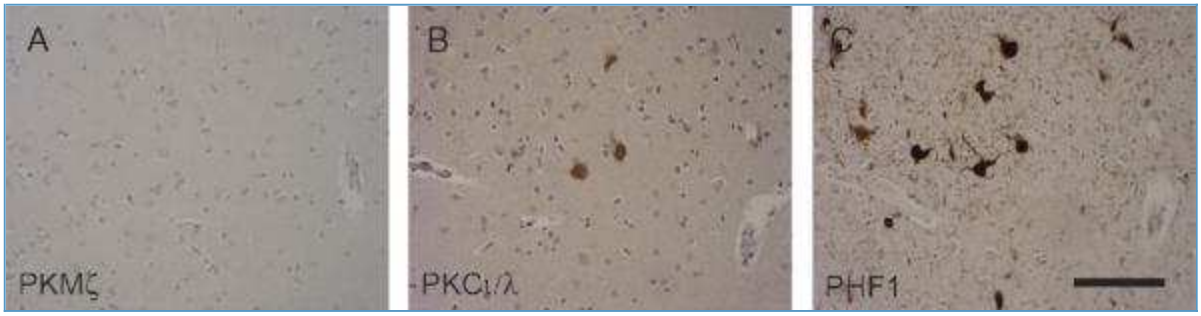

FIGURE 7. Neurofibrillary tangles (NFTs) within entorhinal cortex in a 69-year-old man without Alzheimer disease reveal PKC[iota]/[lambda] but not PKM[zeta] immunoreactivity. PKM[zeta] antisera fails to label any NFTs **(A)**, whereas several NFTs are labeled by PKC[iota]/[lambda] immunohistochemistry **(B)** in serial sections containing many PHF1-positive NFTs **(C)**. Scale bar = 100 μm.

DISCUSSION

We have shown that, within the family of PKC isoforms, only PKC[iota]/[lambda] and PKM[zeta] are present in NFTs in AD. Furthermore, whereas PKC[iota]/[lambda] antisera label NFTs in multiple sites in AD, PKM[zeta]-positive NFTs are restricted to medial temporal lobe structures associated with memory function. This regional specificity is intriguing in view of the role of PKM[zeta] in the maintenance of synaptic plasticity in animal models of memory (6) and contrasts with the usual widespread distribution of tangle-associated proteins (e.g. tau and other tau-associated kinases) in AD. This unusual topographic pattern of PKM[zeta]-positive NFTs cannot be explained on the basis of selective expression of this molecule within these limbic structures, because PKM[zeta] is widely expressed in the forebrain of rodents (10) and humans (Fig. 1). Although there is no clear explanation for this observation, it is possible that increased PKM[zeta] synthesis occurring during LTP (10) renders those neurons actively involved in memory such as hippocampal pyramidal cells especially vulnerable to PKM [zeta] aggregation. This aggregation may contribute to the pathophysiological basis of memory impairment in AD.

Another unusual finding is the absence of PKM[zeta]-positive NFTs in limbic or medial temporal lobe regions in the brains of 5 elderly individuals without AD (Fig. 7). Although modest numbers of NFTs, some immunopositive for PKC[iota]/[lambda], were present in hippocampus and entorhinal cortex in these control cases, PKM[zeta] was absent in these tangle-bearing neurons. This observation is unexpected given that the properties of NFTs in aged, nondemented individuals generally recapitulate those found in NFTs in AD. This intriguing finding further strengthens the link between PKM[zeta] aggregation and memory loss and warrants additional study and confirmation.

Additionally, we found PKM[zeta] within perisomatic granules in association with

AMPA receptors, key molecules in the expression of LTP (25). AMPA receptors have been demonstrated within perisomatic granules, ubiquitin-containing structures variably associated with Hirano body filaments described in AD and other conditions (23, 24). The coexistence of PKM[zeta] and AMPA receptors within perisomatic granules and abnormally distended neurites within medial temporal structures in AD links both molecules to the dysfunction of synaptic plasticity believed to be important in the disease.

Unlike other kinases that have been associated with NFTs, PKM[zeta] is autonomously active, an essential property enabling this enzyme to maintain the long-term enhancement of synaptic transmission during LTP (6). The sequestration of PKM [zeta] within medial temporal tangles may inhibit the normal activity of this kinase in modulating the trafficking of AMPA receptors at synapses. Together, our data suggest that disruption of the normal function of PKM[zeta] in maintaining LTP may contribute to memory loss in AD. Investigation into the mechanism of PKM[zeta] aggregation may provide a new target for treatment of AD.

ACKNOWLEDGMENTS

The authors thank Dr. Marla Gearing of the Emory Alzheimer's Disease Center, Atlanta, Georgia, and Dr. David Bennett of the Rush Alzheimer's Disease Center, Chicago, Illinois, for providing autopsy brain tissue from AD and control cases. The authors also thank the patients and staff of both centers. Dr. Peter Davies generously shared the PHF1 antisera. Lorraine Braithwaite-Harte, William Oxberry, and Andrew Tcherepanov provided excellent technical assistance.

REFERENCES

1. Braak H, Braak E. Neuropathological stageing of Alzheimer-related changes. Acta Neuropathol (Berl) 1991;82:239-59 **Bibliographic Links** | [Context Link]

2. Arriagada PV, Growdon JH, Hedley-Whyte ET, Hyman BT. Neurofibrillary tangles but not senile plaques parallel duration and severity of Alzheimer's disease. Neurology 1992;42:631-39 **Bibliographic Links** | [Context Link]

3. Mann DM, Esiri MM. The site of the earliest lesions of Alzheimer's disease. N Engl J Med 1988;318:789-90 [Context Link]

4. Selkoe DJ. Alzheimer's disease is a synaptic failure. Science 2002;298:789-91 [Context

Link]

5. Lisman J. Long-term potentiation: Outstanding questions and attempted synthesis. Philos Trans R Soc Lond B Biol Sci 2003;358:829-42 **Bibliographic Links** | [Context Link]

6. Ling DS, Benardo LS, Serrano PA, et al. Protein kinase Mzeta is necessary and sufficient for LTP maintenance. Nat Neurosci 2002;5:295-96 [Context Link]

7. Kofler K, Erdel M, Utermann G, Baier G. Molecular genetics and structural genomics of the human protein kinase C gene module. Genome Biol 2002;3research 0014. 1-research 0014. 10 [Context Link]

8. Newton AC. Regulation of the ABC kinases by phosphorylation: Protein kinase C as a paradigm. Biochem J 2003;370:361-71 **Bibliographic Links** | [Context Link]

9. Marshall BS, Price G, Powell CT. Rat protein kinase c zeta gene contains alternative promoters for generation of dual transcripts with 5'-end heterogeneity. DNA Cell Biol 2000;19:707-19 **Bibliographic Links** | [Context Link]

10. Hernandez AI, Blace N, Crary JF, et al. PKMzeta synthesis from a brain mRNA encoding an independent PKCzeta catalytic domain: Implications for the molecular mechanism of memory. J Biol Chem 2003;278:40305-316 [Context Link]

11. Muslimov IA, Nimmrich V, Hernandez AI, Tcherepanov A, Sacktor TC, Tiedge H. Dendritic transport and localization of protein kinase Mzeta mRNA: Implications for molecular memory consolidation. J Biol Chem 2004;279:52613-22 [Context Link]

12. Serrano P, Yao Y, Sacktor TC. Persistent phosphorylation by protein kinase Mzeta maintains late-phase long-term potentiation. J Neurosci 2005;25:1979-84 **Bibliographic Links** | [Context Link]

13. Ling DS, Bernardo LS, Sacktor TC. Protein kinase Mzeta enhances excitatory synaptic transmission by increasing the number of active postsynaptic AMPA receptor. Hippocampus, in press [Context Link]

14. Drier EA, Tello MK, Cowan M, et al. Memory enhancement and formation by atypical PKM activity in *Drosophila melanogaster*. Nat Neurosci 2002;5:316-24 [Context Link]

15. Masliah E, Cole G, Shimohama S, et al. Differential involvement of protein kinase C isozymes in Alzheimer's disease. J Neurosci 1990;10:2113-24 **Bibliographic Links** | [Context Link]

16. Clark EA, Leach KL, Trojanowski JQ, Lee VM. Characterization and differential distribution of the three major human protein kinase C isozymes (PKC alpha, PKC beta, and PKC gamma) of the central nervous system in normal and Alzheimer's disease brains. Lab Invest 1991;64:35-44 **Bibliographic Links** | [Context Link]

17. Shao CY, Crary JF, Rao C, Sacktor TC, Mirra SS. Atypical protein kinase C in neurodegenerative disorders II: iota/lambda in tauopathies and alpha-synucleinopathies. J Neuropathol Exp Neurol 2006 [Context Link]

18. Sacktor TC, Osten P, Valsamis H, Jiang X, Naik MU, Sublette E. Persistent activation of the zeta isoform of protein kinase C in the maintenance of long-term potentiation. Proc Natl Acad Sci U S A 1993;90:8342-46 **Bibliographic Links** | [Context Link]

19. Naik MU, Benedikz E, Hernandez I, et al. Distribution of protein kinase Mzeta and the complete protein kinase C isoform family in rat brain. J Comp Neurol 2000;426:243-58 [Context Link]

20. Mirra SS, Heyman A, McKeel D, et al. The consortium to establish a registry for Alzheimer's disease (CERAD). II Part, standardization of the neuropathologic assessment of Alzheimer's disease. Neurology 1991;41:479-86 **Bibliographic Links** | [Context Link]

21. Consensus recommendations for the postmortem diagnosis of Alzheimer's disease. The National Institute on Aging, and Reagan Institute Working Group on Diagnostic Criteria for the Neuropathological Assessment of Alzheimer's Disease. Neurobiol Aging 1997;18:S1-2 [Context Link]

22. Romijn HJ, van Uum JF, Breedijk I, EmmeringJ, Radu I, Pool CW. Double immunolabeling of neuropeptides in the human hypothalamus as analyzed by confocal laser scanning fluorescence microscopy. J Histochem Cytochem 1999;47:229-36 [Context Link]

23. Probst A, Herzig MC, Mistl C, Ipsen S, Tolnay M. Perisomatic granules (non-plaque dystrophic dendrites) of hippocampal CA1 neurons in Alzheimer's disease and Pick's

disease: A lesion distinct from granulovacuolar degeneration. Acta Neuropathol (Berl) 2001;102:636-44 **Bibliographic Links** | [Context Link]

24. Aronica E, Dickson DW, Kress Y, Morrison JH, Zukin RS. Non-plaque dystrophic dendrites in Alzheimer hippocampus: A new pathological structure revealed by glutamate receptor immunocytochemistry. Neuroscience 1998;82:979-91 **Bibliographic Links** | [Context Link]

25. Nicoll RA. Expression mechanisms underlying long-term potentiation: A postsynaptic view. Philos Trans R Soc Lond B Biol Sci 2003;358:721-26 **Bibliographic Links** | [Context Link]

28. Greenberg SG, Davies P, Schein JD, Binder LI. Hydrofluoric acid-treated tau PHF proteins display the same biochemical properties as normal tau. J Biol Chem 1992;267:564-69 [Context Link]

Key Words: Alzheimer disease; AMPA receptor; Atypical protein kinase C; Memory; Neurofibrillary tangle; Perisomatic granule; Synaptic plasticity

---

IMAGE GALLERY

Select All Export Selected to PowerPoint

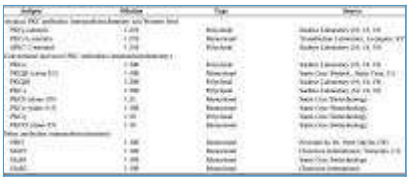

Table 1

Case No.	Age	Sex	Braak Stage (I)	Diagnosis	Postmortem Interval (hr)
1	60	F	VI	AD	NA
2	72	F	VI	AD	4.0
3	82	M	V	AD	2.5
4	70	F	V	AD	1.5
5	86	F	V	AD	6.5
6	91	F	IV/V	AD	3.0
7	83	F	IV	AD	3.5
8	83	F	IV	AD	14.0
9	65	M	III–IV	Control	12.0
10	96	F	III–IV	Control	NA
11	66	F	II	Control	NA
12	69	M	II	Control	6.0
13	98	M	II	Control	NA
14	60	F	I	Control	8.0

NA, not available; AD, cases meeting neuropathologic criteria for Alzheimer disease (20, 21); Control, no known history of dementia without neuropathologic criteria for Alzheimer disease.

Table 2

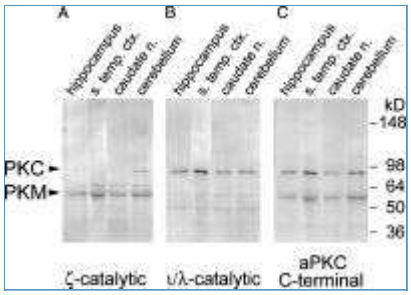

Figure 1

	PKMζ	PKCι/λ
CA1/subiculum	12% ± 15	44% ± 24
Entorhinal cortex	24% ± 30	72% ± 14
Amygdala	25% ± 36	50% ± 24
Middle frontal cortex	Rare	81% ± 33
Superior temporal cortex	Rare	78% ± 18

*, Mean percentage ± standard error of the mean.

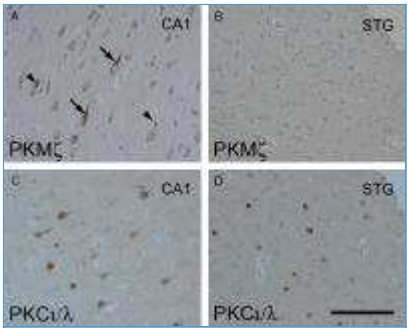

Figure 2

	Case No.							
	1	2	3	4	5	6	7	8
Limbic system								
CA1	+	+	+	−	+	+	+	+
Subiculum	+	+	+	−	+	+	−	+
Entorhinal Cortex	+	+	−	−	−	+	−	+
Amygdala	+	+	+	+	−	+	NA	+
Projection nuclei								
Nucleus basalis	−	−	−	−	−	−	−	−
Dorsal raphe	−	−	NA	−	−	−	−	−
Locus caeruleus	−	−	−	−	−	−	−	−
Cerebral cortex								
Frontal	−	−	−	−	−	−	−	−
Temporal	−	−	−	−	−	−	−	−
Parietal	−	−	−	−	−	−	−	−
Occipital	−	−	−	−	−	−	−	−

NA, not available; (+/−) indicates the presence or absence of PKM[zeta]-positive neurofibrillary tangles.

Table 3

Table 4

Figure 3

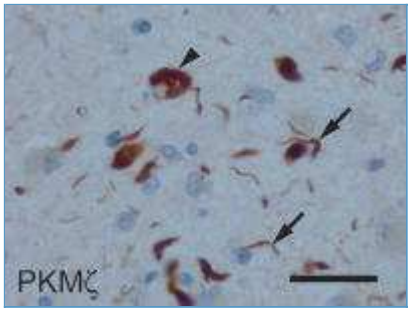

Figure 4

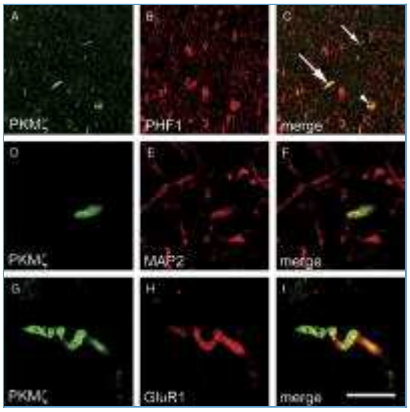

Figure 5

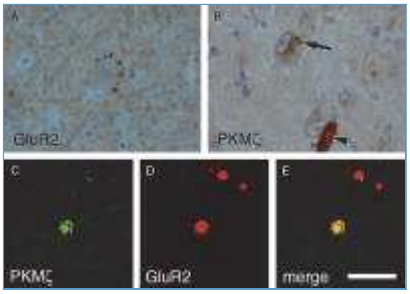

Figure 6

Figure 7

Back to Top